Journal of Materials Chemistry

Cite this: J. Mater. Chem., 2012, 22, 232

www.rsc.org/materials

PAPER

Luminogenic materials constructed from tetraphenylethene building blocks: Synthesis, aggregation-induced emission, two-photon absorption, light refraction, and explosive detection†

Rongrong Hu,[a] Jose Luis Maldonado,[b] Mario Rodriguez,[b] Chunmei Deng,[a] Cathy K. W. Jim,[a] Jacky W. Y. Lam,[a] Matthew M. F. Yuen,[d] Gabriel Ramos-Ortiz*[b] and Ben Zhong Tang*[ac]

Received 26th July 2011, Accepted 27th September 2011
DOI: 10.1039/c1jm13556b

Luminogenic molecules [$(TPE)_3$ (**1**), TPE-C = C-TPE-C = C-TPE (**2**), and TPE-C≡C-TPE-C≡C-TPE (**3**)] and their polymers **P1–P3** are constructed from tetraphenylethene (TPE) building blocks in high yields by Suzuki, Witting, and Sonogashira coupling reactions. All the compounds are soluble and enjoy high thermal stability, losing little of their weights when they are heated to 290–528 °C under nitrogen or 288–436 °C in air. Analyses by UV spectroscopy and cyclic voltammetry as well as theoretical calculations show that the conjugation of the luminophores is in the order of **2** > **3** > **1**, **P2** > **P3** > **P1**, and **P1–P3** > **1–3**. All the molecules and polymers are weakly emissive in solutions. They, however, become strong emitters in the aggregate state with fluorescence quantum yields up to 90%. Both **1–3** and **P1–P3** exhibit the feature of aggregation-enhanced two-photon excited fluorescence. Large two-photon absorption cross sections (up to ~900 GM) are observed in the nanoaggregates of the polymers. Thin solid films of the polymers show high refractive indices (RI = 1.7649 − 1.6873) in a wide wavelength region of 400–1700 nm, high modified Abbé numbers (v_D' up to 3436), and low optical dispersions (D' down to 2.9×10^{-4}). The light emissions of the polymers can be quenched exponentially by picric acid with large quenching constants, suggesting that they can be utilized as efficient chemosensors for explosive detection.

Introduction

Materials with two-photon absorption (TPA) have drawn much attention in recent years given their exceptional utility in three-dimensional micro fabrication and storage,[1] optical power limiting,[2] three-dimensional imaging,[3] photodynamic therapy,[4] and two-photon pumped up-converted lasers.[5] To realize the full potential of the TPA technology, new TPA materials with large TPA cross sections and good processability, photostability, and durability are needed.[6] Thanks to the research efforts of scientists, a number of organic TPA materials with varied molecular structures have been prepared, which provides insight into their structure-property relationship and gives valuable information for further molecular design and synthesis. For example, compounds with higher conjugation have been found to exhibit larger TPA cross sections. Incorporation of electron-donating and accepting units into the molecular structures also helps enhance the absorption. Other factors such as molecular coplanarity, solvent polarity, and hydrogen-bonding are found to play constructive effects in the enhancement of the TPA cross section.[7]

For biophotonic applications, the TPA dyes should possess good water solubility or dispersity and remain highly fluorescent in aqueous media. However, many of them suffer the aggregation-caused emission quenching effect in concentrated solutions or in aqueous media owing to their hydrophobic nature and strong π–π interaction, which has somewhat limited their practical applications.[8] To alleviate such problems, scientists utilized polymer nanoparticles as biocompatible encapsulating carriers to achieve a stable dispersion of the hydrophobic dyes. A challenge remaining to be solved in this methodology is the inevitable dilution of the active dye in a nanoparticle carrier, which cannot

[a]*Department of Chemistry, The Hong Kong University of Science & Technology, Clear Water Bay, Kowloon, Hong Kong, China. E-mail: tangbenz@ust.hk*
[b]*Centro de Investigaciones en Óptica, A. P. 1-948, 37000 León, Gto, México. E-mail: garamoso@cio.mx*
[c]*Department of Polymer Science and Engineering, Institute of Biomedical Macromolecules, Key Laboratory of Macromolecular Synthesis and Functionalization of the Ministry of Education, Zhejiang University, Hangzhou, China*
[d]*Department of Mechanical Engineering, The Hong Kong University of Science & Technology, Clear Water Bay, Kowloon, Hong Kong, China*

† Electronic supplementary information (ESI) available: Synthesis and characterizations; high resolution mass spectra of **1–3**; photographs of **2**, **3**, **P2**, and **P3** in THF and THF/water mixtures taken under UV illumination and their associated emission spectra, molecular orbital plots of HOMO and LUMO energy levels of *cis* **1–3**; emission spectra of **P1** in THF and THF/water mixtures (1/1 v/v) containing different amounts of picric acid. See DOI: 10.1039/c1jm13556b

be offset by increasing the dye loading because of the notorious aggregation-caused quenching (ACQ) effect.[9] With such regard, fabrication of silica nanoparticles[10] and polyion complexation[11] have been proposed as alternative tools to enhance the organo-modified fluorescence and TPA cross section of the luminophors in the aggregate state.

Recently, we and other groups observed a phenomenon of aggregation-induced emission (AIE) that is exactly opposite to the ACQ effect: a series of propeller-shaped molecules are non-emissive in solutions but are induced to emit intensely by aggregate formation.[12] Such a novel effect enables the AIE luminogens to find potential high-tech applications as chemo-sensors, bioprobes, immunoassay markers, stimuli-responsive materials, and solid-state emitters. Although AIE luminogens with various functionalities have been prepared, there are few examples available in the literature that report the synthesis of luminogenic compounds with both AIE features and TPA absorption.[13] Collini and coworkers reported the enhancement of TPA cross section of a fluorescent tetrakis(4-sulfonatophenyl) porphyrin diacid in the aggregate state.[14] Prasad and coworkers reported the aggregation-enhanced emission and two photon absorption in nanoaggregates of 9,10-bis[4′-(4″-aminostyryl) styryl]anthracene derivatives.[15]

To overcome the ACQ limitation of the current TPA luminophors, in this paper, we aim to synthesise AIE luminogens with nonlinear optical properties. We chose tetraphenylethene (TPE), an archetypal AIE luminogen, as a building block because of its facile synthesis, ready functionalization, and high quantum yield. We linked TPE units by different functional bridge groups and generated molecules **1–3** and polymers **P1–P3** with different conjugations (Chart 1). We aim to investigate how conjugation affects their properties such as light emission and TPA absorption and meanwhile explore their potential practical applications.

Experimental section

Materials

Tetrahydrofuran (THF) and toluene were distilled under normal pressure from sodium benzophenone ketyl under argon immediately prior to use. Dimethylformamide (DMF) and triethylamine (Et_3N) were distilled and dried over potassium hydroxide. Rhodamine 6G was purchased from Exciton Inc. Dichloromethane (DCM), diphenylmethane (**4**), 4-bromobenzophenone (**5**), *n*-butyllithium (*n*-BuLi), dichlorobis(triphenylphosphine)palladium(II) [$Pd(PPh_3)_2Cl_2$], copper(I) iodide (CuI), triphenylphosphine (PPh_3), zinc powder, titanium(IV) chloride ($TiCl_4$), tetrabutylammonium fluoride (TBAF), *p*-toluenesulfonic acid (PTSA), trimethyl borate [$B(OCH_3)_3$], sodium carbonate (Na_2CO_3), tetrakis(triphenylphosphine)palladium(0) [$Pd(PPh_3)_4$], *N*-bromosuccinimide (NBS), benzoyl peroxide (BPO), *N*-formylpiperidine, potassium *tert*-butoxide (*t*-BuOK), trimethylsilylacetylene, and other chemicals and solvents were all purchased from Aldrich and used as received without further purification. Compound **7**, named 1-(4-bromophenyl)-1,2,2-triphenylethene, was synthesized according to the literature method.[16]

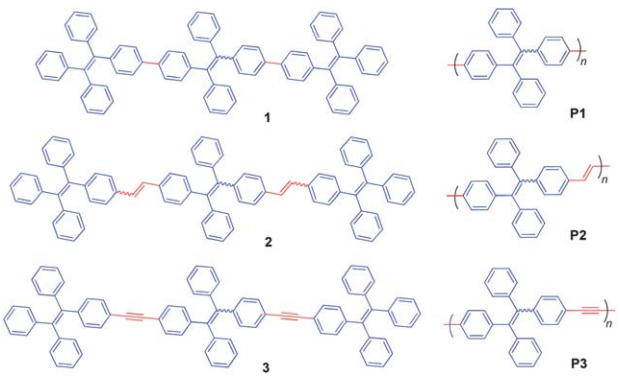

Chart 1 Molecular structures of the tetraphenylethylene-containing molecules and polymers.

Instruments

^1H and ^{13}C NMR spectra were measured on Bruker ARX 300 or 400 NMR spectrometers using $CDCl_3$ or CD_2Cl_2 as solvents and tetramethylsilane (TMS; $\delta = 0$ ppm) as internal standard. IR spectra were recorded on a Perkin-Elmer 16 PC FT-IR spectrophotometer. Thermogravimetric analysis (TGA) was carried out under nitrogen or in air on a Perkin-Elmer TGA 7 analyzer at a heating rate of 10 °C min^{-1}. UV-vis absorption spectra were measured on a Milton Roy Spectronic 3000 array spectrophotometer. Photoluminescence (PL) spectra were recorded on a Perkin-Elmer LS 55 spectrofluorometer. The fluorescence quantum yields of **1–3** and **P1–P3** in THF (2.6 μM) and their nanoaggregates dispersed in water were determined by using an integrating sphere calibrated by a fluorescent standard (Rhodamine 6G) with known quantum yield. A HeCd laser (325 nm) was employed as excitation source. The number (M_n) and weight-average (M_w) molecular weights and polydispersity indices (PDI or M_w/M_n) of the polymers were estimated by a Waters Associates gel permeation chromatography (GPC) system equipped with RI and UV detectors. THF was used as eluent at a flow rate of 1.0 mL. A set of monodisperse linear polystyrenes covering the molecular weight range of 10^3–10^7 were used as standards for the calibration. High resolution mass spectra were recorded on a GCT premier CAB048 mass spectrometer operating in a MALDI-TOF mode. Cyclic voltammetry was conducted on a CHI600A electrochemical workstation. All the measurements were carried out at room temperature using a conventional three-electrode configuration at a scan rate of 100 mV s^{-1}. The working electrode was a glassy carbon electrode with a diameter of 2 mm. Silver chloride electrode was used as reference and the counter electrode was a platinum wire. The solutions were prepared in distilled DCM. Tetrabutylammonium hexafluorophosphate (0.1 M) was used as supporting electrolyte. The refractive indices of the polymers were determined on a J A Woollam variable angle ellipometry system with a wavelength tunability from 300 to 1700 nm. To fit the acquired Ψ and Δ curves with the data obtained from the 3-layer optical model consisting of a crystalline silicon substrate, 2-nm SiO_2 layer and a uniform polymer film, the Levenberg-Marquardt regression algorithm was employed. The Cauchy dispersion law was applied to describe the polymer layer from the visible to IR spectral region. The ground state geometries of **1–3** were optimized *via* density functional theory (DFT). The DFT calculations were carried out using the B3LYP

functional, where Becke's three-parameter hybrid exchange functional was combined with the Lee–Yang–Parr correlation functional,[17] and a def2-SV(P) basis set.[18] All calculations were performed with the TURBOMOLE 6.0 program.[19]

Two-photon absorption (TPA) of the molecules and polymers in the solution and aggregate states was measured by the two-photon excited fluorescence (TPEF) technique using a Ti: Sapphire laser (Spectra-Physics). This laser provided pulses of 100 fs of duration at a repetition rate of 80 MHz and was tunable in the wavelength range of 740–820 nm. The laser beam was focused into a quartz cell of 1 cm path length by using a 5 cm focal-length lens. A half-wave plate and a polarizer were used to control the excitation intensity. The induced two-photon fluorescence was collimated by a lens at a direction perpendicular to the pump beam. To minimize the attenuation of fluorescence due to linear absorption effects, the excitation beam was focused as close as possible to the lateral wall of the quartz cell. The TPEF was then focused into the input slit of an imaging spectrograph and recorded at the exit with a CCD camera. To calculate the TPEF cross sections, Rhodamine 6G in methanol solution (10 μM) and its nanoaggregates were utilized as references for the calculation. All the samples and standards were tested under the same experimental conditions. The TPEF cross sections were calculated by the equation: $\sigma_{TPEF} = \sigma_{ref}\, c_{ref}\, n_{ref}\, F/cnF_{ref}$, where c and n were the concentration and refractive index of the samples and reference, and F was the integral of the TPEF spectrum. The two photon cross section σ_{TPA} was then calculated by the equation $\sigma_{TPA} = \sigma_{TPEF}/\Phi_F$, where Φ_F was the fluorescence quantum yield of the sample as stated in Table 1.

Synthesis

Compound **1–3** and polymer **P1–P3** were prepared according to the synthetic routes shown in Scheme 1 and 2. Detailed procedures and characterization can be found in the supporting information.

Preparation of aggregates

Stock THF solutions of the molecules and polymers with a concentration of 0.1 mM were prepared. An aliquot (1 mL) of this stock solution was transferred to a 10 mL volumetric flask. After adding an appropriate amount of THF, water was added dropwise under vigorous stirring to furnish 10 μM THF/water mixtures with water fractions (f_w) of 0–90 vol %. 10 μM THF/water mixtures with 95% water contents were prepared by 1 mM THF solutions in the same manner. The absorption and emission spectra of the resultant mixtures were measured immediately.

Table 1 Optical properties of **1–3** and **P1–P3**[a]

Compound	λ_{ab} (nm)	λ_{em} (nm)	Φ_{soln} (%)	Φ_{aggr} (%)
1	341	493	1.0	90
2	360	511	1.0	76
3	352	500	0.5	74
P1	356	506	1.2	28
P2	382	520	3.4	64
P3	360	502	1.1	18

[a] Abbreviation: λ_{ab} = absorption maximum in THF solution (10 μM), λ_{em} = emission maximum in THF/water mixture (1 : 9 v/v), Φ_{soln} and Φ_{aggr} = fluorescence quantum yields in THF and aqueous nanoparticle suspension determined by an calibrated integrating sphere.

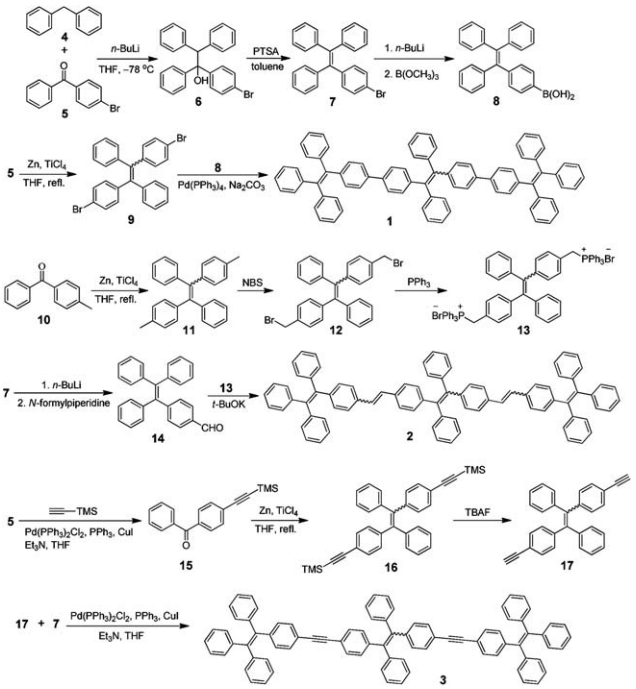

Scheme 1 Synthetic routes for compounds **1–3**.

The nanoaggregates used in the TPA cross section measurement were prepared by the reprecipitation method. First, solutions of **1–3** and **P1–P3** were prepared by dissolving 1 mg of the compounds in 2 mL THF. 0.5 mL of each solution was then injected quickly into 8 mL of poor solvent (aqueous solution of cetyl trimethyl ammonium bromide, 0.08 mM). After sonication, THF was partially removed under vacuum. Through such a procedure, the concentrations of the nanoparticle suspensions were in the range of 2×10^{-7} to 3×10^{-5} M.

Explosive detection

A stock solution of picric acid (PA) with a concentration of 2 mg mL^{-1} was prepared by dissolving an appropriate amount of PA in THF. Photoluminescence titration was carried out by adding

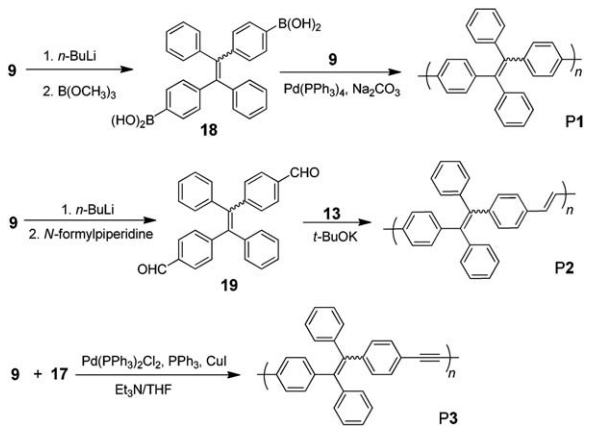

Scheme 2 Synthesis of polymers **P1–P3**.

aliquots of PA solution into solutions of **P1** in THF and THF/water mixtures with 50 and 90% water contents.

Results and discussion

Synthesis

To endow the AIE luminogens with new functionalities and widen their practical applications, we designed the molecular structures of a group of luminogenic molecules (**1–3**) and polymers (**P1–P3**) and elaborated multi-step reaction routes for their syntheses (Scheme 1 and 2). Lithiation of **4** followed by reaction with **5** generated **6**, which underwent dehydration in the presence of PTSA to form **7** in 95% yield. Treatment of **7** with *n*-butyllithium followed by reaction with trimethyl borate furnished **8**. Meanwhile, McMurry coupling reaction of **5** catalyzed by $TiCl_4$/Zn produced **9** with both *cis* and *trans* isomers, whose palladium-catalyzed Suzuki coupling with **8** gave **1** in 62% yield.

Similarly, McMurry coupling reaction of **10** afforded **11**, which was converted into **12** by bromination with NBS. Reaction of **12** with triphenylphosphine generated phosphonium salt. On the other hand, lithiation of **7** followed by addition of *N*-formylpiperidine furnished **14**. Witting reaction of **13** and **14** in the presence of potassium *tert*-butoxide afforded **2** in 91% yield. Meanwhile, palladium-catalyzed Sonogashira coupling reaction of **5** with trimethylsilylacetylene produced **15**, whose McMurry coupling reaction generated **16**. Desilylation of **16** yielded **17** and its coupling reaction afforded the desirable product **3** in 95% yield.

To prepare the polymeric analogs of **1–3**, **9** was converted into diboronic acid **18** and dialdehyde **19** by lithiation followed by reaction with trimethyl borate and *N*-formylpiperidine, respectively. Polymerizations of **9/18** and **13/19** pairs under the conditions for Suzuki and Witting reactions generated **P1** and **P2** in high yields with moderate molecular weights. On the other hand, Sonogashira coupling of **9** with **17** furnished **P3** again in a high isolated yield.

Structural characterization

All the intermediates and products were characterized by standard spectroscopic methods and all gave satisfactory analysis data corresponding to their expected molecular structures (see experimental section for details). Luminogens **1–3**, for example, give M^+ peaks at *m*/*z* 992.4176 (calcd for **1**, 992.4382), 1044.6278 (calcd for **2**, 1044.4695), and 1040.4373 (calcd for **3**, 1040.4382) in their HRMS spectra (Fig. S1–S3†), confirming the formation of the expected products. The IR spectra of **9**, **17**, and **P3** are also given in Fig. 1 as an example. The spectrum of **P3** resembles its monomers but exhibits no ≡C–H and terminal C≡C stretching vibrations of **17** at 3281 and 2107 cm^{-1}, respectively, suggesting that all the molecules of **17** have been consumed by the polymerization reaction.

Analysis by ^1H NMR spectroscopy gives similar results. The acetylene proton resonance of **17** occurs at δ 3.09, which is absent in the spectrum of **P3** (Fig. 2). The absorptions of the aromatic protons in **P3** are broad because its TPE units are knitted together by rigid acetylene linkages.

The ^{13}C NMR spectra of **9**, **17**, and their polymer **P3** are shown in Fig. 3. The spectrum of **P3** shows no resonance peaks of

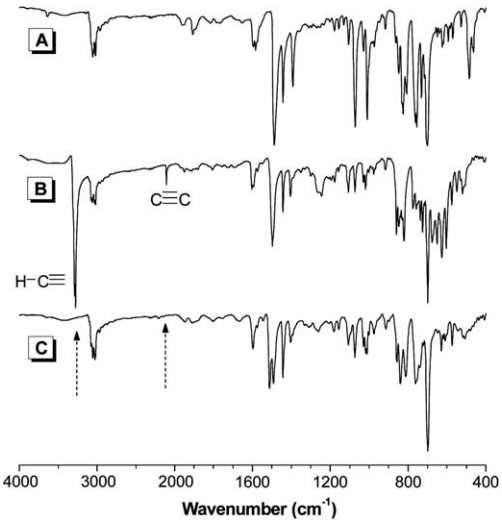

Fig. 1 IR spectra of (A) **9**, (B) **17**, and (C) their polymer **P3**.

carbon atoms of **17** at δ 78.1 and 84.2. A new peak associated with the absorptions of the internal triple bond carbons was observed at δ 90.4. No other unexpected signals are found, revealing that the polymeric product is indeed **P3**, with a molecular structure as shown in Chart 1.

Solubility and stability

Though **1–3** and **P1–P3** are constructed from aromatic rings, they dissolve readily in common organic solvents, such as toluene, dichloromethane, chloroform, and THF. Polymers **P1–P3** can also form tough films by spin-coating their solutions. The good solubility of the molecules and polymers may be stemmed from the twisted conformation of their TPE units, which reduces intermolecular interactions and generates large free volume to accommodate more solvent molecules.

Since **1–3** and **P1–P3** possess many aromatic rings, they are anticipated to show high resistance to thermolysis.[20] This is indeed the case, as revealed by their TGA thermograms shown in

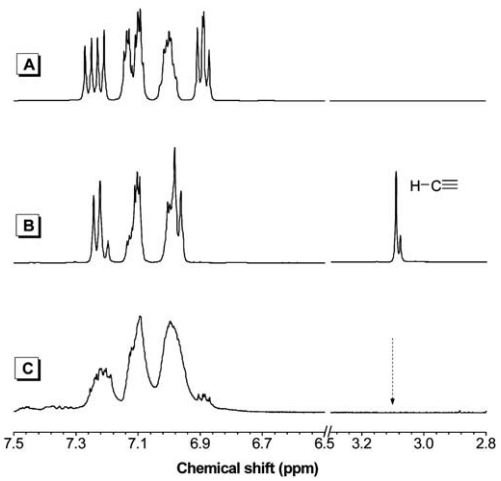

Fig. 2 ^1H NMR spectra of (A) **9**, (B) **17**, and (C) their polymer **P3** in dichloromethane-d_2.

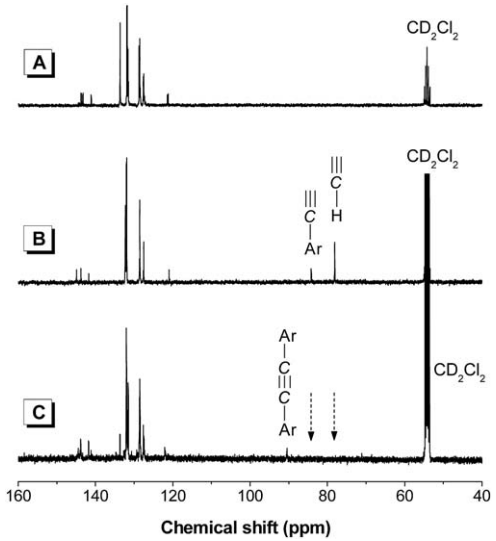

Fig. 3 ^{13}C NMR spectra of (A) **9**, (B) **17**, and (C) their polymer **P3** in dichloromethane-d_2.

Fig. 4. Molecules **1–3** show 5% of their weight loss (T_d) at 290–308 °C under nitrogen atmosphere. Similar T_d values are recorded when the measurements are performed in air. Compared to their low molecular weight counterparts, **P1–P3** enjoy higher thermal stability. They start to decompose at higher temperatures with T_d values of 463–528 °C under nitrogen. Although they exhibit lower thermal stability in air, their T_d values are all beyond 430 °C and still much higher than those of **1–3**. It is noteworthy that more than 70% of their weights are retained when they are heated under nitrogen at 600 °C, making them promising as precursors for ceramic materials.

Photophysical properties

The absorption spectra of **1–3** and **P1–P3** in their dilute THF solutions are depicted in Fig. 5. The absorption spectra of **1–3** peaked at 341, 360, and 352 nm, respectively, revealing that the functional bridge group has influenced strongly the conjugation of the molecules. The absorption maxima of **P1–P3** are located at 356, 382, and 360 nm, which are 15, 22, and 8 nm red-shifted from those of **1–3**, indicative of a higher conjugation in the polymeric system.

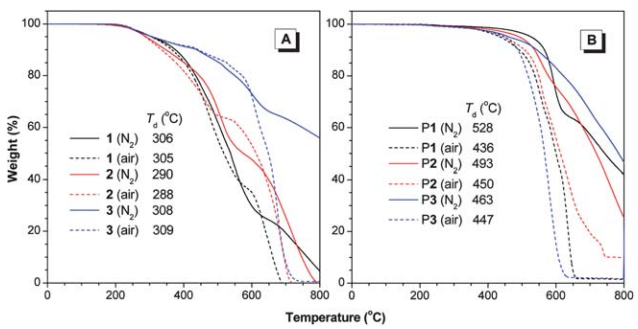

Fig. 4 TGA thermograms of (A) **1–3** and (B) **P1–P3** recorded under nitrogen and in air at a heating rate of 10 °C min^{-1}.

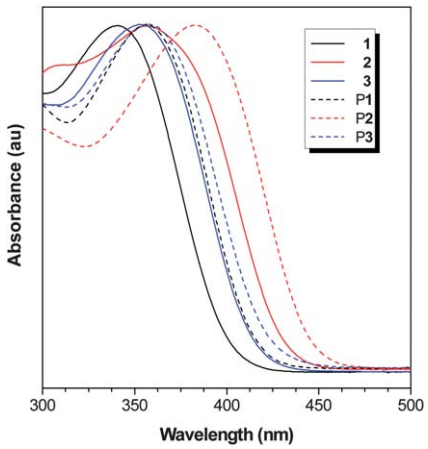

Fig. 5 Normalized absorption spectra of **1–3** and **P1–P3** in THF solutions. Concentration: 10 μM.

All the molecules and polymers, similar to TPE, are AIE-active, as suggested by the fluorescent images of their solutions in THF and THF/water mixtures. The photographs of solutions of **1** and **P1** are given in Fig. 6 and 7 as examples, while those of **2**, **3**, **P2**, and **P3** are provided in Fig. S4–S7†. The THF solution of **1** emits no light under UV illumination. Addition of a poor solvent such as water into the THF solution has, however, aggregated its molecules and enhanced its emission intensity. The emission is still weak in aqueous mixtures at low water fractions (≤50%) but becomes stronger afterwards. A similar phenomenon was also observed in **P1** but its solution is already somewhat emissive in the presence of a small amount of water (30%), presumably due to its comparatively lower solubility in the aqueous mixture.

In addition to the visual observations, we also studied the emission behaviors of **1–3** and **P1–P3** in the solution and aggregate states by using a spectrofluorometer. As shown in Fig. 6B, **1** is practically non-emissive in THF. When 60% of water

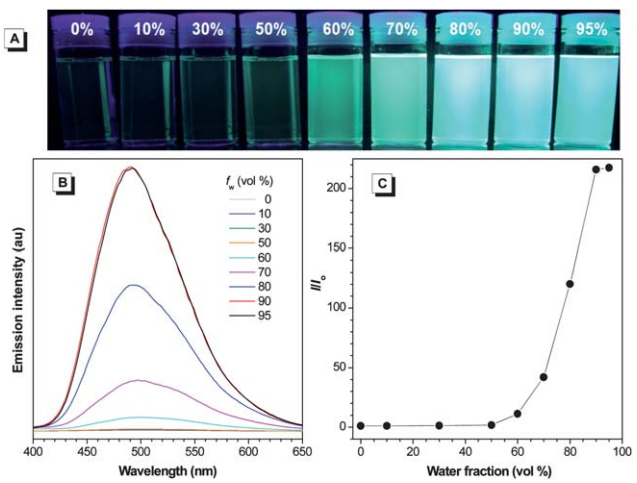

Fig. 6 (A) Photographs of **1** in THF/water mixtures with different fractions of water (f_w) taken under UV illumination. (B) Emission spectra of **1** in THF/water mixtures. (C) Plot of (I/I_o) values *versus* the compositions of the aqueous mixtures. I_o = emission intensity in pure THF solution. Solution concentration: 10 μM; excitation wavelength: 341 nm.

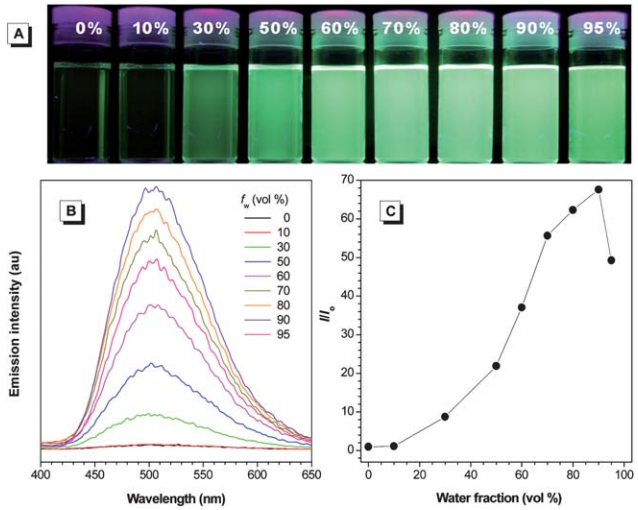

Fig. 7 (A) Photographs of **P1** in THF/water mixtures with different fractions of water (f_w) taken under UV illumination. (B) Emission spectra of **P1** in THF/water mixtures. (C) Plot of (I/I_o) values *versus* the compositions of the aqueous mixtures. I_o = emission intensity in pure THF solution. Solution concentration: 10 μM; excitation wavelength: 356 nm.

is added to its THF solution, an emission peak, however, emerges at 493 nm, whose intensity is enhanced by further increasing the water content in the aqueous mixture. From the isolated species in THF solution to nanoaggregates in 90% aqueous mixture, the emission intensity rises by 216-fold (Fig. 6C). Unlike **1**, **P1** emits at 506 nm in pure THF solution albeit in a low intensity (Fig. 7B). We have previously proposed that the AIE phenomenon is caused by the restriction of intramolecular rotation in the aggregate state, which blocks the nonradiative relaxation channel and populates the radiative decay. The TPE units in **P1** are knitted together by covalent bonds, which partially restricts their intramolecular rotation and hence makes the polymer somewhat emissive in the solution state. The emission intensity starts to rise when a small amount of water is added to the THF solution and reaches its maximum value at 90% water content, which is 68-fold higher than that in pure THF solution (Fig. 7C). Similar observations are also found in **2**, **3**, **P2**, and **P3** (Fig. S4–S7†).

To have a quantitative comparison, we measured the fluorescence quantum yields (Φ_F) of the molecules and polymers in the solution and aggregate states. Whereas the Φ_F values of **1–3** in THF are generally below 1%, those in the aggregate state are much higher (74–90%), manifesting their AIE feature (Table 1). The Φ_F values of **P1–P3** in the solution state are also low (1.1–3.4%) but in relative terms, they are higher than those of **1–3**, in agreement with their stronger emissions in the THF solutions. The polymers show higher fluorescence quantum yields in the aggregated state. Compared with those of **1–3**, their Φ_F values, however, are much lower, probably due to the emission quenching caused by the defects in the polymer chain.

Electronic structure

To better understand the photophysical properties of **1–3**, theoretical calculations on their energy levels were performed. The molecular orbital amplitude plots of the HOMO and LUMO energy levels of *trans* **1–3** are shown in Fig. 8, while those of the *cis* counterparts are provided in Fig. S8†. All the *trans* isomers show similar orbital distribution and their HOMO and LUMO energy levels are dominated by the central TPE core and the vinyl cores of the two terminal TPE units. The six peripheral phenyl rings are twisted and contribute little to the energy levels of the molecules. This orbital distribution results in a linear and high conjugation in **1–3**. The two peripheral TPE units are also conjugated with the central TPE core in *cis* **1–3**. The orbitals of their HOMO and LUMO, however, are distributed in a V-shaped manner. The calculated HOMO and LUMO values of the *cis* and *trans* isomers are almost the same (Table S1†), indicating that their mixing would not affect the overall photophysical properties of the molecules. The calculated energy band gaps for *trans* **1**, **2** and **3** are 3.53, 3.05, and 3.20 eV, respectively, which nicely explain the bathochromic shifts in the absorption and emission of **2** from those of **3** and **1**.

Electrochemical properties

We also investigated the electrochemical properties of **1–3** by cyclic voltammetry. Such a method is widely used for estimating the energy levels of organic semiconductors. All the molecules exhibit similar voltammograms. Their HOMO energy levels can be estimated from their onset oxidation potentials based on the value of −4.8 eV for ferrocene as internal standard with respect to the zero vacuum level. The onset oxidation potentials of **1–3** are found at 1.14, 1.14, and 1.21 eV from which HOMO values of −5.45, −5.45, and −5.52, are derived, respectively (Table 2). The band gaps of **1–3** can be determined from their onset absorption wavelengths and are calculated to be 3.11, 2.89, and 3.00 eV, respectively. Although the experimental values are somewhat lower than the calculated ones, the conjugation of the molecules is still in the order of **2** > **3** > **1**.

Nonlinear optical properties

Since **1–3** and **P1–P3** are conjugated, we are intrigued to know whether they show two-photon excited fluorescence and absorption. With this in mind, we thus investigated the nonlinear optical properties of the molecules and polymers in the solution and aggregate states by a two-photon excited technique.

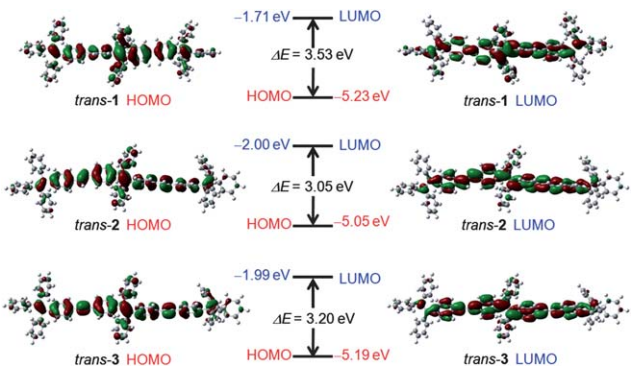

Fig. 8 Molecular orbital amplitude plots of HOMO and LUMO energy levels of *trans* **1–3** calculated using B3LYP/6-31G(d) basis set.

Table 2 Electrochemical and optical properties of **1–3**[a]

Compound	$E_{onset\text{-}ox}$ (V)	HOMO (eV)	λ_{onset}(nm)	E_g(eV)	LUMO (eV)
1	1.14	−5.45	399	3.11	−2.34
2	1.14	−5.45	429	2.89	−2.56
3	1.21	−5.52	414	3.00	−2.52

[a] Abbreviation: $E_{onset\text{-}ox}$ = onset oxidation potential measured by cyclic voltammetry, HOMO = highest occupied molecular orbital derived by the equation: HOMO = $-(E_{onset\text{-}ox} + 4.8 - E_{ferrocene})$ eV, where the value of $E_{ferrocene}$ measured in our experiment was 0.49 eV, λ_{onset} = onset absorption wavelength, E_g = energy band gap determined from λ_{onset}, LUMO = lowest unoccupied molecular orbital = E_g + HOMO.

Delightfully, all the molecules and polymers exhibit two-photon excited fluorescence (TPEF). An example of the TPEF spectra of **P2** in THF and aqueous nanoparticle suspension are given in Fig. 9. Both the spectra peaked at 520 nm. The TPEF intensity of the latter, however, is 8.6-fold higher than the former, demonstrating of a phenomenon of aggregation enhanced two-photon excited fluorescence.

The two-photon absorption cross sections (σ_{TPA}) of the molecules and polymers are given in Table 3. The σ_{TPA} values of **1–3** are low in THF (0.5–4.7 GM) when photoexcited at 800 nm. On the contrary, **P1–P3** exhibit much higher absorptions under the same experimental conditions, presumably due to their higher conjugation. All the compounds show higher σ_{TPA} values in the aggregate state, particularly for **P2**, which absorbs intensely with a σ_{TPA} value of 275.8 GM. Their AIE effect can be compared by using the γ_{AIE} value, which is defined by the equation: $\gamma_{AIE} = \sigma_{TPA,\ aggr}/\sigma_{TPA,\ soln}$. The γ_{AIE} values of **1–3** range from 1.4 to 2.8, while those of **P1–P3** reach 8.7, 8.7, and 7.5, respectively, which are larger than the values of most compounds reported previously.[13,15,21]

Since **1–3** and **P1–P3** show no absorption or weakly absorb at 800 nm, one would expect they show stronger TPEF and higher TPA values at shorter excitation wavelengths. Indeed, the σ_{TPA} values of the molecules and polymers are much higher (enhancement up to 10-fold) when determined at 750 nm excitation wavelength. Again, the nanoaggregates show larger TPA cross sections than their corresponding isolated species in THF solutions. The σ_{TPA} values of **P2** and **P3** are impressively high (895.9 GM for **P2** and 714.2 GM for **P3**) with γ_{AIE} values larger than 8, taking into the account that the absorptions of most TPA materials in the aggregate state lie in the range of 90–330 GM.[10,11,13–15,21] This is quite unusual because **P2** and **P3** possess no electron-donating or accepting unit in their molecular structures and compounds with similar structures normally have low σ_{TPA} values. For example, the σ_{TPA} value of stilbene is merely 12 GM.[7b]

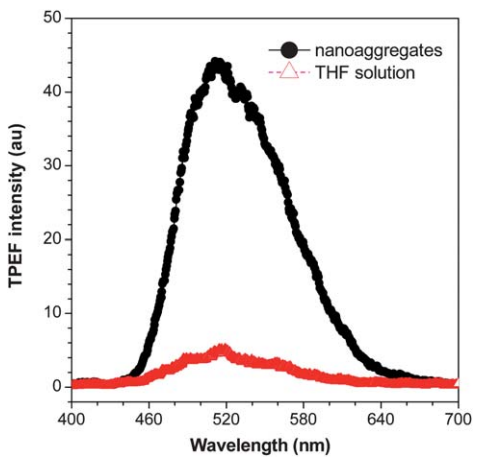

Fig. 9 TPEF spectra of THF solution and nanoaggregates of **P2**. Solution concentration: 2.6 mM; excitation wavelength: 800 nm.

Preliminary results show that the σ_{TPA} values of the molecules and polymers are further enhanced if lower excitation wavelengths are used. For example, the σ_{TPA} value for the nanoaggregates of **P2** determined at 740 nm excitation wavelength is as high as 1360.9 GM. A more detailed investigation on the TPA properties of the compounds is under investigation. It is noteworthy that the light emissions of the nanoaggregates are very stable, suffering no spectral change when they are dispersed in the aqueous nanoparticle suspension for several months. This enables them to find potential biophotonic applications, for example, as markers for multiphoton microscopy or biosensors.

Light refraction

P1–P3 are conjugated and possess many aromatic rings and thus may show high refractive indices (RI). Indeed, as can be seen from Fig. 10, the thin film of **P2** prepared by spin-coating of its solution displays high RI values ($n = 1.7649 - 1.6873$) in a wide wavelength region (400–1700 nm). Similarly high RI values are also observed in **P3** ($n = 1.7795 - 1.6430$). The RI values of **P2** and **P3** at 632.8 nm are ≥1.69, which is much higher than those of the commercially important optical plastics (*e.g.*, $n \sim 1.49$ for PMMA).

For a material to be useful for practical applications, its optical aberrations should be small. The Abbé number (ν_D) of a material is a measure of the variation or dispersion in its RI value with wavelength and is defined as: $\nu_D = (n_D - 1)/(n_F - n_C)$, where n_D, n_F and n_C are the RI values at wavelengths of Fraunhofer D, F and C spectral lines of 589.2, 486.1 and 656.3 nm, respectively. A modified Abbé number (ν_D') has also been proposed to evaluate the potential application of an optical material, using its RI values at the non-absorbing wavelengths of 1064, 1319 and 1550 nm.[22] The modified Abbé number is defined as: $\nu_D' = (n_{1319} - 1)/(n_{1064} - n_{1550})$, where n_{1319}, n_{1064} and n_{1550} are the RI values at 1319, 1064 and 1550 nm, respectively. The chromatic dispersion (D') is the constringence of the Abbé number: ($D' = 1/\nu_D'$). Both **P2** and **P3** show low optical dispersions. The D value of **P2** is 36.0×10^{-3}, which is comparable to those of the commercially important "organic glasses" such as PC ($D = 29.7 \times 10^{-3}$) and PMMA ($D = 17.5 \times 10^{-3}$).

Table 3 Two-photon absorption of **1–3** and **P1–P3** in the solution (soln)[a] and aggregated (aggr)[b] states[c]

	$\lambda_{ex,\ 800\ nm}$			$\lambda_{ex,\ 750\ nm}$		
Compound	$\sigma_{TPA,\ soln}$(GM)	$\sigma_{TPA,\ aggr}$(GM)	γ_{AIE}	$\sigma_{TPA,\ soln}$ (GM)	$\sigma_{TPA,\ aggr}$ (GM)	γ_{AIE}
1	0.5	1.4	2.8	nd	2.9	nd
2	4.7	13.2	2.8	49.1	63.9	1.3
3	1.9	2.7	1.4	nd	8.7	nd
P1	2.1	18.2	8.7	nd	56.5	nd
P2	31.7	275.8	8.7	106.9	895.9	8.4
P3	20.8	155.7	7.5	88.7	714.2	8.1

[a] In THF solution (2.6 μM). [b] In aqueous nanoparticle suspension (31.25 μg mL^{-1}). [c] Abbreviation: λ_{ex} = excitation wavelength, σ_{TPA} = two-photon absorption cross section, $\gamma_{AIE} = \sigma_{TPA,\ aggr}/\sigma_{TPA,\ soln}$, nd = not determined because of the weak excitation intensity at 750 nm.

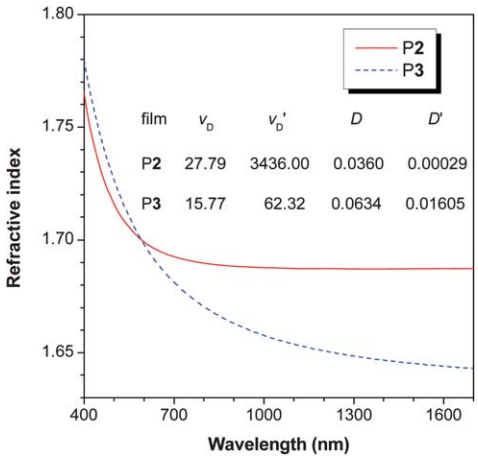

Fig. 10 Wavelength dependence of refractive index of thin films of **P2** and **P3**.

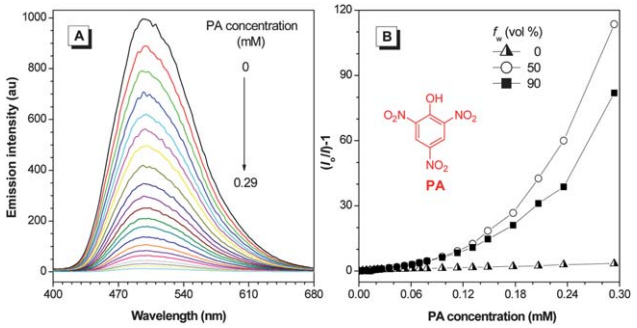

Fig. 11 (A) Emission spectra of **P1** in THF/water mixture with 90% water fraction (f_w) containing different amounts of picric acid (PA). (B) Plots of ($I_o/I - 1$) values *versus* PA concentrations in THF/water mixtures with f_ws of 0, 50, and 90 vol%. I_o = intensity at [PA] = 0 mM. Concentration: 10 mM; excitation wavelength: 356 nm.

Explosive detection

Sensors based on fluorescent conjugated polymers have attracted much attention due to their amplified response and superior sensitivity to analytes, in comparison to their low molar mass congeners. Generally, intrinsic autoaggregation of chains of conjugated polymers and/or their analyte-induced aggregation causes self-quenching problems that greatly reduce the sensing performance. However, aggregation is beneficial to the emission of **P1–P3**. With such regard, we explored their utility as chemosensors for explosives because their sensitive detection has antiterrorism implications.[23] The nanoaggregates of **P1** in THF/water mixtures with 50 and 90% water contents are utilized as probes. For comparison, the detection was also carried out in pure THF solution. Picric acid (PA) was employed as a model compound due to its commercial availability.

As shown in Fig. 11A, the emission of **P1** is weakened when PA is gradually added into its nanoaggregates in the aqueous mixture. The fluorescence quenching can be clearly discerned at a PA concentration as low as 1 ppm. At a PA concentration of 0.29 mM, virtually no light can be detected by the spectrofluorometer. The Lewis acid–base interactions between the TPE units of **P1** with the electron-deficient PA molecules may play a key role in the quenching process. The Stern–Volmer plot of relative PL intensity ($I_o/I - 1$) *versus* PA concentration in THF solution as well as the nanoaggregates suspended in the aqueous mixtures give curves bending upward instead of linear lines (Fig. 11B), indicating that the PL quenching becomes more efficient with increasing quencher concentration. The emission of the aggregates decreases in a much faster rate than their isolated chains in THF solution (Fig. S9†), indicative of a higher sensitivity. The nanoaggregates have more cavities to bind with more quencher molecules and provide additional interchain diffusion pathways for excitons to migrate,[24] thus making the quenching a highly efficient process. The aggregate-based sensor in the aqueous mixture with $f_w = 50\%$ shows a higher sensing performance than that with $f_w = 90\%$, probably because the polymer packing in the former is looser than in the latter and the looser packing allows voids to interact with more PA molecules.

Conclusions

In this work, luminogenic molecules (**1–3**) and polymers (**P1–P3**) are synthesized in high yields from tetraphenylethene building blocks by Suzuki, Witting, and Sonogashira coupling reactions. All the compounds are soluble and show high thermal stability, losing little of their weights when they are heated to 290–528 °C under nitrogen or 288–436 °C in air. UV and CV analyses as well as theoretical calculations demonstrate that the conjugation of the molecules and polymers is in the order of **2** > **3** > **1**, **P2** > **P3**> **P1**, and **P1–P3** > **1–3**. Whereas both **1–3** and **P1–P3** are weakly

emissive in solutions, they become strong emitters when aggregated in poor solvent with fluorescence quantum yields up to 90%, demonstrative of a phenomenon of aggregation-induced emission. Both molecules and polymers exhibit the feature of aggregation-enhanced two-photon excited fluorescence. Large two-photon absorption cross sections (up to ~900 GM) are observed in the nanoaggregates of **P1–P3**, whose values can be further enhanced by using an excitation source of shorter wavelengths. Thin solid films of **P2** and **P3** show high refractive indices (RI = 1.7649 − 1.6873) in a wide wavelength region of 400–1700 nm, high modified Abbé numbers, and low optical dispersions. The light emission of **P1** can be quenched efficiently by picric acid with a large quenching constant. Materials with such attributes are anticipated to find an array of high-tech applications.

Acknowledgements

This work was partially supported by the Research Project Competition of HKUST (RPC11SC09 and RPC10SC13), the Research Grants Council of Hong Kong (604711, 603509, HKUST2/CRF/10), the University Grants Committee of Hong Kong (AoE/P-03/08), and the National Science Foundation of China (20634020 and 20974028). B. Z. T. is thankful for the support from Cao Guangbiao Foundation of Zhejiang University. Gabriel Ramos-Ortiz is thankful for the CONACYT grant (grant J49512F).

References

1 (*a*) G. S. He, T. S. Tan, Q. D. Zheng and P. N. Prasad, *Chem. Rev.*, 2008, **108**, 1245; (*b*) S. Kawata and Y. Kawata, *Chem. Rev.*, 2000, **100**, 1777; (*c*) D. A. Parthenopoulos and P. E. Rentzepis, *Science*, 1989, **245**, 843; (*d*) S. Kawata, H. B. Sun, T. Tanaka and K. Takada, *Nature*, 2001, **412**, 697; (*e*) B. H. Cumpston, S. P. Ananthavel, S. Barlow, D. L. Dyer, J. E. Ehrlich, L. L. Erskine, A. A. Heikal, S. M. Kuebler, I. Y. S. Lee, D. McCord-Maughon, J. Qin, H. Rockel, M. Rumi, X. L. Wu, S. R. Marder and J. W. Perry, *Nature*, 1999, **398**, 51; (*f*) H. B. Sun, T. Kawakami, Y. Xu, J. Y. Ye, S. Matuso, H. Misawa, M. Miwa and R. Kaneko, *Opt. Lett.*, 2000, **25**, 1110; (*g*) W. H. Teh, U. During, G. Salis, R. Harbers, U. Drechsler, R. F. Mahrt, C. G. Smith and H. J. Guntherodt, *Appl. Phys. Lett.*, 2004, **84**, 4095; (*h*) A. S. Dvornikov, E. P. Walker and P. M. Rentzepis, *J. Phys. Chem. A*, 2009, **113**, 13633.

2 (*a*) A. C. Walker, A. K. Kar, W. Ji, U. Keller and S. D. Smith, *Appl. Phys. Lett.*, 1986, **48**, 683; (*b*) E. W. Van Stryland, Y. Y. Wu, D. J. Hagan, M. J. Soileau and K. Mansour, *J. Opt. Soc. Am. B*, 1988, **5**, 1980; (*c*) P. A. Bouit, G. Wetzel, G. Berginc, B. Loiseaux, L. Toupet, P. Feneyrou, Y. Bretonniére, K. Kamada, O. Maury and C. Andraud, *Chem. Mater.*, 2007, **19**, 5325; (*d*) Y. Morel, A. Irimia, P. Najechalski, Y. Kervella, O. Stephan, P. L. Baldeck and C. Andraud, *J. Chem. Phys.*, 2001, **114**, 5391; (*e*) N. Venkatram, D. N. Rao and M. A. Akundi, *Opt. Express*, 2005, **13**, 867.

3 (*a*) W. Denk, J. H. Strickler and W. W. Webb, *Science*, 1990, **248**, 73; (*b*) D. R. Larson, W. R. Zipfel, R. M. Williams, S. W. Clark, M. P. Bruchez, F. W. Wise and W. W. Webb, *Science*, 2003, **300**, 1434; (*c*) D. J. Bharali, D. W. Lucey, H. Jayakumar, H. E. Pudavar and P. N. Prasad, *J. Am. Chem. Soc.*, 2005, **127**, 11364.

4 (*a*) J. P. Celli, B. Q. Spring, I. Rizvi, C. L. Evans, K. S. Samkoe, S. Verma, B. W. Pogue and T. Hasan, *Chem. Rev.*, 2010, **110**, 2795; (*b*) H. Stiel, K. Teuchner, A. Paul, W. Freyer and D. Leupold, *J. Photochem. Photobiol., A*, 1994, **80**, 289.

5 A. Mukherjee, *Appl. Phys. Lett.*, 1993, **62**, 3423.

6 B. A. Reinhardt, L. L. Brott, S. J. Clarson, A. G. Dillard, J. C. Bhatt, R. Kannan, L. X. Yuan, G. S. He and P. N. Prasad, *Chem. Mater.*, 1998, **10**, 1863.

7 (*a*) H. M. Kim and B. R. Cho, *Chem. Commun.*, 2009, 153; (*b*) M. Albota, D. Beljonne, J. L. Bredas, J. E. Ehrlich, J. Y. Fu, A. A. Heikal, S. E. Hess, T. Kogej, M. D. Levin, S. R. Marder, D. McCord-Maughon, J. W. Perry, H. Rockel, M. Rumi, G. Subramaniam, W. W. Webb, X. L. Wu and C. Xu, *Science*, 1998, **281**, 1653.

8 (*a*) J. B. Birks, *Photophysics of Aromatic Molecules*, Wiley, Chichester, UK 1970; (*b*) W. S. Li and T. Aida, *Chem. Rev.*, 2009, **109**, 6047; (*c*) B. Gu, W. Ji, X. Q. Huang, P. S. Patil and S. M. Dharmaprakash, *J. Appl. Phys.*, 2009, **106**, 33511.

9 (*a*) A. Mishra, C. Q. Ma and P. Bäuerle, *Chem. Rev.*, 2009, **109**, 1141; (*b*) A. C. Grimsdale, K. L. Chan, R. E. Martin, P. G. Jokisz and A. B. Holmes, *Chem. Rev.*, 2009, **109**, 897.

10 (*a*) L. Li, Y. Tian, J. Yang, P. Sun, L. Kong, J. Wu, H. Zhou, S. Zhang, B. Jin, X. Tao and M. Jiang, *Chem. Commun.*, 2010, **46**, 1673; (*b*) S. Kim, Q. D. Zheng, G. S. He, D. J. Bharali, H. E. Pudavar, A. Baev and P. N. Prasad, *Adv. Funct. Mater.*, 2006, **16**, 2317.

11 N. Kato, Y. Katayama, H. Semba and K. Limura, *Jpn. J. Appl. Phys.*, 2010, **49**, 031601.

12 (*a*) J. Luo, J. W. Y. Lam, L. Cheng, H. Chen, C. Qiu, H. S. Kwok, X. Zhan, Y. Liu, D. Zhu and B. Z. Tang, *Chem. Commun.*, 2001, 1740; (*b*) Y. Hong, J. W. Y. Lam and B. Z. Tang, *Chem. Commun.*, 2009, 4332; (*c*) D. Oelkrug, A. Tompert, J. Gierschner, H. J. Egelhaaf, M. Hanack, M. Hohloch and E. Steinhuber, *J. Phys. Chem. B*, 1998, **102**, 1902; (*d*) D. Oelkrug, A. Tompert, H. J. Egelhaaf, M. Hanack, E. Steinhuber, m. Hohloch, H. Meier and U. Stalmach, *Synth. Met.*, 1996, **83**, 231; (*e*) M. K. Chaudhuri and S. C. Ganguly, *J. Phys. C: Solid State Phys.*, 1969, **2**, 1560; (*f*) T. Ikeyama and T. Azumi, *J. Phys. Chem.*, 1985, **89**, 5332.

13 (*a*) H. H. Fang, Q. D. Chen, J. Yang, H. Xia, B. R. Gao, J. Feng, Y. G. Ma and H. B. Sun, *J. Phys. Chem. C*, 2010, **114**, 11958; (*b*) Y. H. Jiang, Y. C. Wang, J. L. Hua, J. Tang, B. Li, S. X. Qian and H. Tian, *Chem. Commun.*, 2010, **46**, 4689.

14 E. Collini, C. Ferrante and R. Bozio, *J. Phys. Chem. B*, 2005, **109**, 2.

15 (*a*) S. Kim, T. Y. Ohulchanskyy, H. E. Pudavar, R. K. Pandey and P. N. Prasad, *J. Am. Chem. Soc.*, 2007, **129**, 2669; (*b*) S. Kim, H. E. Pudavar, A. Bonoiu and P. N. Prasad, *Adv. Mater.*, 2007, **19**, 3791; (*c*) S. B. Noh, R. H. Kim, W. J. Kim, S. Kim, K. S. Lee, N. S. Cho, H. K. Shim, H. E. Pudavar and P. N. Prasad, *J. Mater. Chem.*, 2010, **20**, 7422.

16 M. Banerjee, S. J. Emond, S. V. Lindeman and R. Rathore, *J. Org. Chem.*, 2007, **72**, 8054.

17 (*a*) A. D. Becke, *J. Chem. Phys.*, 1993, **98**, 5648; (*b*) C. Lee, W. Yang and R. G. Parr, *Phys. Rev. B*, 1988, **37**, 785.

18 (*a*) A. Schafer, H. Horn and R. Ahlrichs, *J. Chem. Phys.*, 1992, **97**, 2571; (*b*) F. Weigend and R. Ahlrichs, *Phys. Chem. Chem. Phys.*, 2005, **7**, 3297.

19 (*a*) R. Ahlrichs, M. Baer, M. Haeser, H. Horn and C. Koelmel, *Chem. Phys. Lett.*, 1989, **162**, 165; (*b*) O. Treutler and R. Ahlrichs, *J. Chem. Phys.*, 1995, **102**, 346; (*c*) F. Furche and R. Ahlrichs, *J. Chem. Phys.*, 2002, **117**, 7433.

20 (*a*) P. Kundu, K. R. J. Thomas, J. T. Lin, Y. T. Tao and C. H. Chien, *Adv. Funct. Mater.*, 2003, **13**, 445; (*b*) J. Y. Shen, C. Y. Lee, T. H. Huang, J. T. Lin, Y. T. Tao, C. H. Chien and C. Tsai, *J. Mater. Chem.*, 2005, **15**, 2455.

21 (*a*) J. S. Park, R. H. Kim, N. S. Cho, H. K. Shim and K. S. Lee, *J. Nanosci. Nanotechnol.*, 2008, **8**, 4793; (*b*) Z. J. Liu, P. Shao, Z. L. Huang, B. Liu, T. Chen and J. G. Qin, *Chem. Commun.*, 2008, 2260.

22 (*a*) C. J. Yang and S. A. Jenekhe, *Chem. Mater.*, 1995, **7**, 1276; (*b*) C. J. Yang and S. A. Jenekhe, *Chem. Mater.*, 1994, **6**, 196.

23 (*a*) J. C. Sanchez, A. G. Dipasquale, A. L. Rheingold and W. C. Trogler, *Chem. Mater.*, 2007, **19**, 6459; (*b*) H. Sohn, M. J. Sailor, D. Magde and W. C. Trogler, *J. Am. Chem. Soc.*, 2003, **125**, 3821.

24 (*a*) S. W. Thomas III, G. D. Joly and T. M. Swager, *Chem. Rev.*, 2007, **107**, 1339; (*b*) U. H. F. Bunz, *Chem. Rev.*, 2000, **100**, 1605; (*c*) J. Liu, Y. Zhong, P. Lu, Y. Hong, J. W. Y. Lam, F. Mahtab, Y. Yu, K. S. Wong and B. Z. Tang, *Polym. Chem.*, 2010, **1**, 426.

